Electronic Supplementary Material (ESI) for Chemical Communications.

In situ Ga-alloying in germanium nano-twists by the inhibition of fractal growth with fast Li^+-mobility

Zhaoliang Yu, [a] Long Yuan, [a] Yingjin Wei, [b] Haibo Li, *[a] Xiangdong Meng, *[a] Yao Li, *[c] Frank Endres, [d]

[a] Key Laboratory of Functional Materials Physics and Chemistry of the Ministry of Education, Jilin Normal University, Changchun, P. R. China.

[b] Key Laboratory of Physics and Technology for Advanced Batteries (Ministry of Education), College of Physics, Jilin University, Changchun, P. R. China

[c] Center for Composite Materials and Structure, Harbin Institute of Technology, Harbin, P. R. China.

[d] Institute of Electrochemistry, Clausthal University of Technology, Clausthal-Zellerfeld, Germany.

Experimental section

Chemicals and materials. Chemicals of $GaCl_3$ (99.999%) and $GeCl_4$ (99.9999%) were purchased from Alfa Aesar and Guojing-Tec, respecively, which were used as received without further purification or pre-treatment. The ionic liquid [EMIm]Tf_2N (99%) was purchased in the highest available quality from Io-Li-Tec (Germany) and used after drying under vacuum at 100 °C for 24 h to reduce the water content to values of below 2 ppm. Then, the ionic liquid was stored in closed bottles in an argon-filled glove box. Isopropanol and acetone were purchased from Beijing Chemical Works (P. R. China). Indium tin oxide (ITO) substrates (~200 nm thick film of ITO film on soda-lime glass), were purchased from HNXCKJ (P. R. China). Copper foil with 0.02 mm thick was purchased from Jingliang Tongye (P. R. China). Prior to the experiments, the ITO substrates and the Cu foil were cut into 20×25 mm sections. This sections were cleaned by acetone and isopropanol for 10 min in an ultrasonic cleaner, respectively. The copper foil was additionally rinsed with dilute hydrochloric acid to remove the oxide layer.

Electrodeposition system. The working electrodes (WE) in the experiment were ITO and a Cu foil, respectively. A silver wire was used as quasi-reference electrode (RE) and a Pt plate was used as counter electrode (CE). In this electrolyte, a Ag wire gives a sufficiently stable electrode potential. The electrochemical cell was made of polytetrafluoroethylene (PTFE) and clamped over a PTFE-covered viton O-ring onto the substrate, thus giving a final geometric surface area of 1.5 cm^2. The PTFE cell and the O-ring were cleaned in a mixture of 50:50 vol% of concentrated H_2SO_4 and H_2O_2 (35%), followed by refluxing in deionized water. The electrochemical measurements were performed with a Princeton 2273 (Princeton Applied Research) electrochemical workstation controlled by Power CV and Power CORR software. A hot plate was used to heat the solution.

Electrodepostion of Ga-nanosphere seeds. $GaCl_3$ and $GeCl_4$ were added to [EMIm]Tf_2N to form 0.1 M $GaCl_3$ and 0.1 M $GeCl_4$ solution in an argon-filled glovebox (Vigor, SG1200/750TS) with water and oxygen contents of below 2 ppm. Subsequently, the solution was stirred for 12 h at room temperature. 0.87 mL of 0.1 M $GaCl_3$/[EMIm]Tf_2N solution was added to the electrochemical cell. Then, solution temperature was gradually heated to 25, 35, 45 and 55 °C to control the particle size of Ga deposits. Afterward, CV test with 0.1 M $GaCl_3$ was carried out in order to determine the deposition potential of Ga. CV measurements were performed at a scan rate

of 50 mV s^{-1} at the range of -2.5 ~ 2 V on ITO substrate and -2.5 ~ 0 V on Cu foil *vs*. the Ag quasi reference electrode. Then, Ga nanospheres were directly electrodeposited on the ITO/Cu substrate at the reduction peak potential obtained form CV curves.

Electrodeposition of $Ge_{0.90}Ga_{0.10}$ nano-twist. After electrodeposition of Ga nanospheres, the $GaCl_3$/[EMIm]Tf_2N solution was removed from electrochemical cell. Then, $GeCl_4$/[EMIm]Tf_2N solution was added to electrochemical cell, and the solution was heated to 60 °C. CV test of 0.1 M $GeCl_4$ on deposited Ga was applied in order to determine the depostion potential of Ge. Subsequently, Ge was electrodeposited on the deposited Ga at reduction peak potential in the ionic liquid to form $Ge_{0.90}Ga_{0.10}$ nano-twist. After the electrochemical experiments, all samples were immersed and washed in isopropanol to remove the ionic-liquid residues.

Characterization. Field-emission scanning electron microscope (FESEM) images were collected with a JSE-7800F microscope (JEOL, Japan), with an operating voltage of 5 kV and current of 89 pA. The composition of the materials was determined by energy dispersive X-ray spectroscopy (EDX). The crystal structures of the nano-twist were investigated by powder X-ray diffraction (XRD, D/max-2500/PC, Rigaku, Japan), with CuKα radiation at 40 kV and 200 mA. The scan speed was 2°/min and 2θ angle range was 20-80°. The microstructure of nano-twist was measured with a transmission electron microscope (TEM, JEM-2100HR, JEOL, Japan). X-ray photoelectron spectrometer (XPS, ESCALAB 250XI, Thermo Fisher, America) was used to analyze the chemical composition of the nano-twist, Al Kα served as the X-ray excitation source.

Li-ion battery measurement. Coin-type half cells (CR2032 size) were prepared inside of the glovebox, contained a $Ge_{0.90}Ga_{0.10}$ nano-twist electrode, a microporous polyethylene separator, Li metal foil as the counter and reference electrode, and 1 M $LiPF_6$ in ethylene carbonate-diethyl carbonate (EC-DEC; 1:1 vol%) used as electrolyte. For testing, the battery was removed from the glovebox. Galvanostatic discharge/charge test were carried out with a Neware battery test system (CT-4008, Shenzhen, China) between 0.01 and 2 V. The rate capability was tested by discharging and charging the material for 5 cycles at current densities of 0.16, 0.32, 0.8, 1.6, 3.2, 8, and 16 A g^{-1}, and then back to 0.16 A g^{-1}. The electrochemical impedance spectroscopy (EIS) measurements was tested on a Princeton 2273 electrochemical workstation by applying an AC voltage of 5 mV

in the frequency range of 10 mHz to 100 kHz tested at ~25 °C. Cyclic voltammetry was tested in the voltage range of 0.01 to 2 V (*vs* Li/Li^+) at a scan rate of 0.1 mV s^{-1}.

Li-ion diffusion coefficient test.

Calculate based on EIS: The diffusion coefficient of Li^+ in active materials can be calculated using the following equation [S1]:

$$D_{Li}=\frac{1}{2}\left[\left(\frac{V_m}{FA\sigma}\right)\left(\frac{dE}{dx}\right)\right]^2 \quad (1)$$

Where V_m is the molar volume, F is the Faraday constant (96485 C mol^{-1}), A is the electrode area (here 1.5 cm^2), dE/dx is the composition dependence of potential which is estimated from Fig. 3(b). σ is the Warburg factor which is acquired from the slope of *Z'* *vs*. $\omega^{-1/2}$.

Calculate based on CV: The diffusion coefficient of Li^+ in active materials also can be calculated according to Randles-Sevick Equation [S2, S3]:

$$I_p=0.4663nFAC(nFvD_{Li}/RT)^{1/2}=2.69\times10^5n^{3/2}AD_{Li}^{1/2}v^{1/2}C \quad (2)$$

I_p indicates the peak current, n is the number of electrons in the reaction, C is the Li-ion concentration in the electrolyte (mol cm^{-3}), v is the scanning rate (V s^{-1}), R is the gas constant (8.314 J mol^{-1} K^{-1}) and T is the absolute temperature (K). The slope of the linear relationship between I_p and $v^{1/2}$ was used to estimate the diffusion coefficient of lithium ions in the electrode.

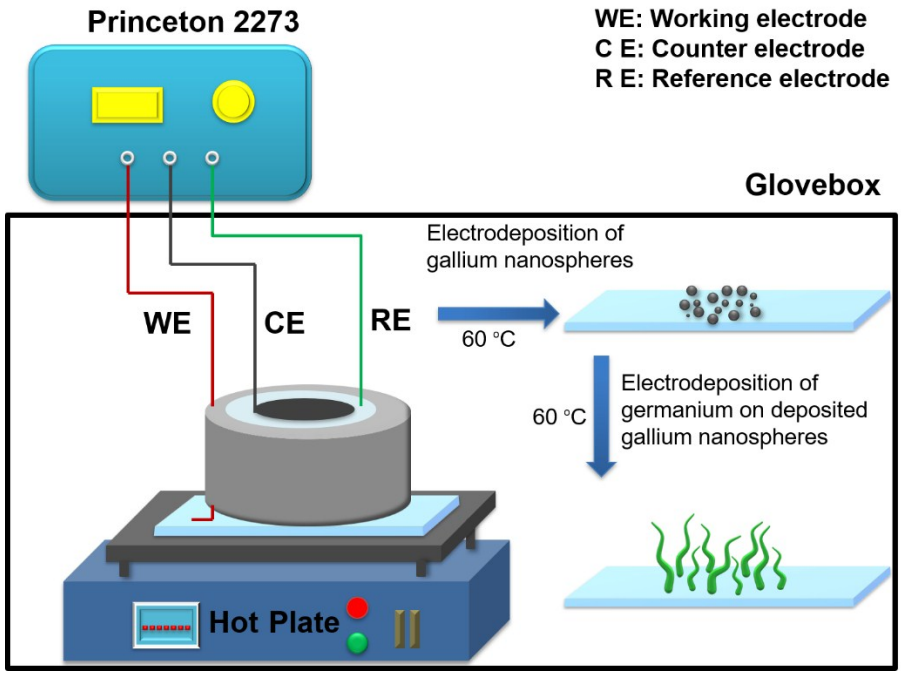

Fig. S1. Equipment of electrodeposition of $Ge_{0.90}Ga_{0.10}$ nano-twist.

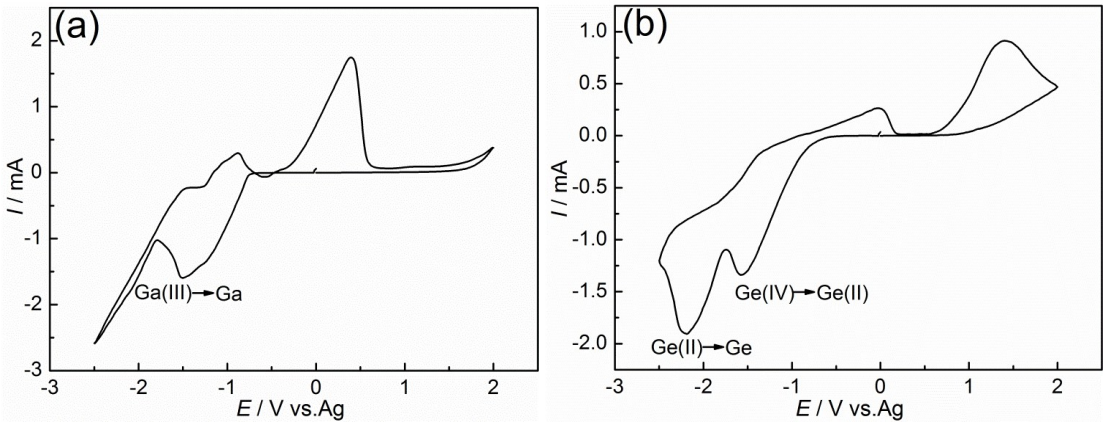

Fig. S2. (a) CV curve of 0.1 M $GaCl_3$ in [EMIm]Tf_2N on the ITO substrate. (b) CV curve of 0.1 M $GeCl_4$ in [EMIm]Tf_2N on the deposited Ga at 60 °C. The scan rate is 50 mV s^{-1}.

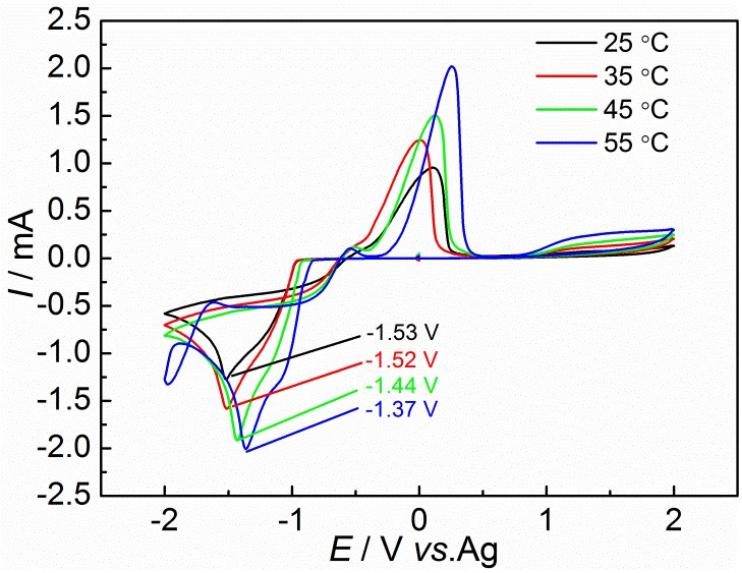

Fig. S3. CV curve of 0.1 M $GaCl_3$ in [EMIm]Tf_2N on ITO acquired at temperature of 25, 35, 45, 55 °C

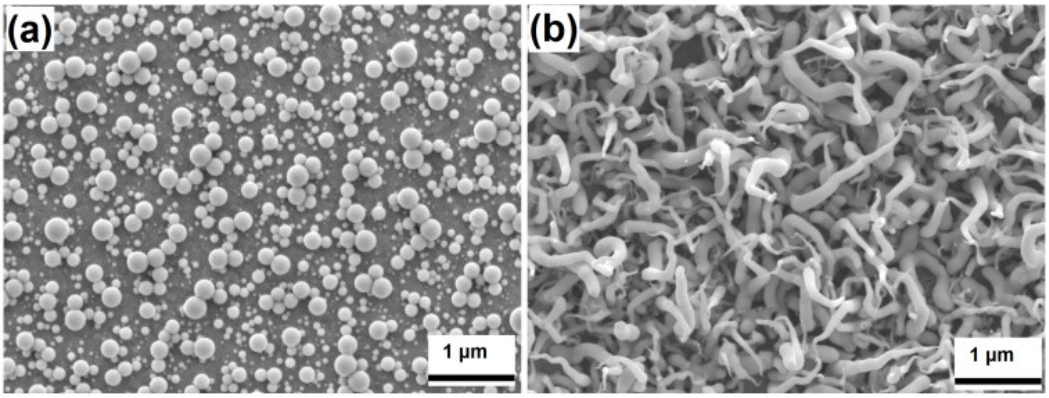

Fig. S4. FESEM images of (a) Ga deposits made for 60 s on the ITO substrate at -1.5 V, (b) $Ge_{0.90}Ga_{0.10}$ nano-twist made at -2.2 V for 300 s on deposited Ga nanosphere.

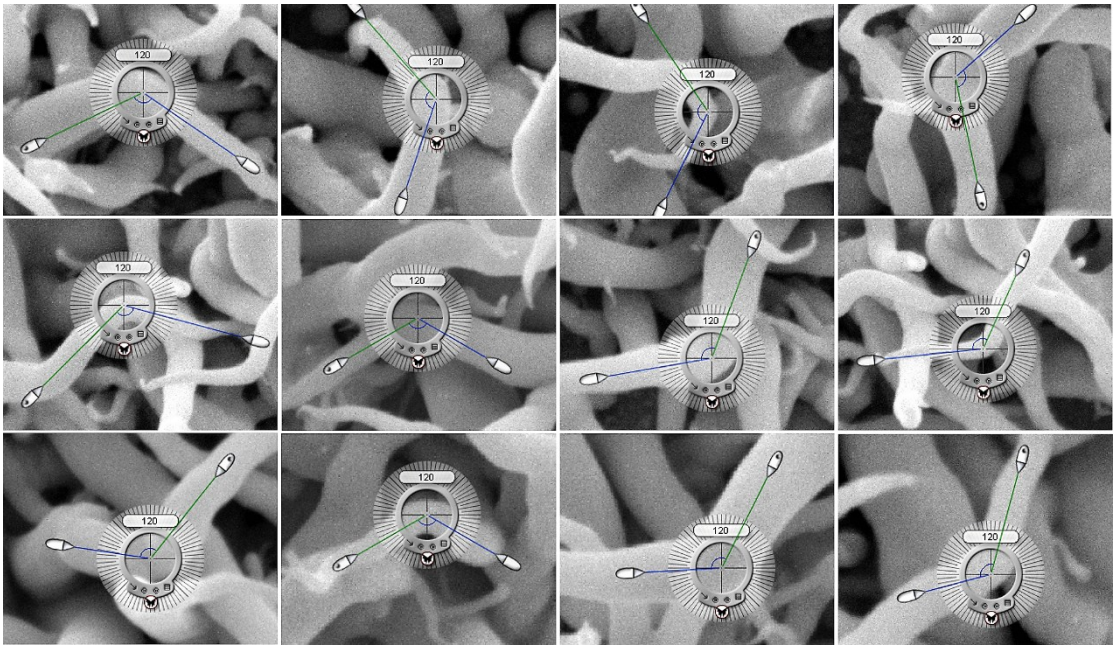

Fig. S5 FESEM images of $Ge_{0.9}Ga_{0.10}$ with 120 º nano-twist.

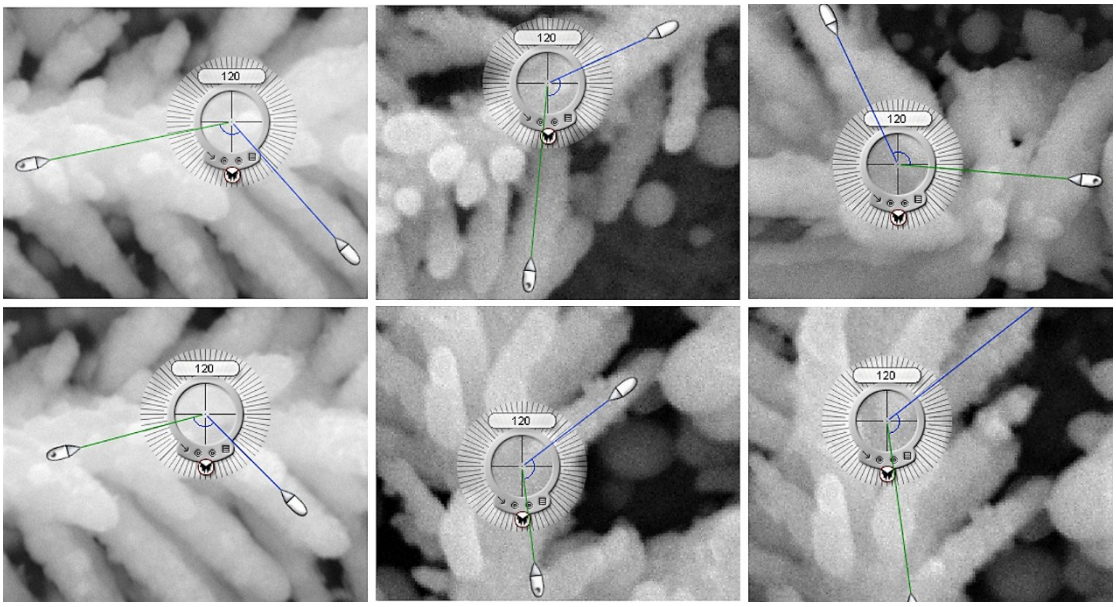

Fig. S6. FESEM images of Ge nano-tree with 120 º branches.

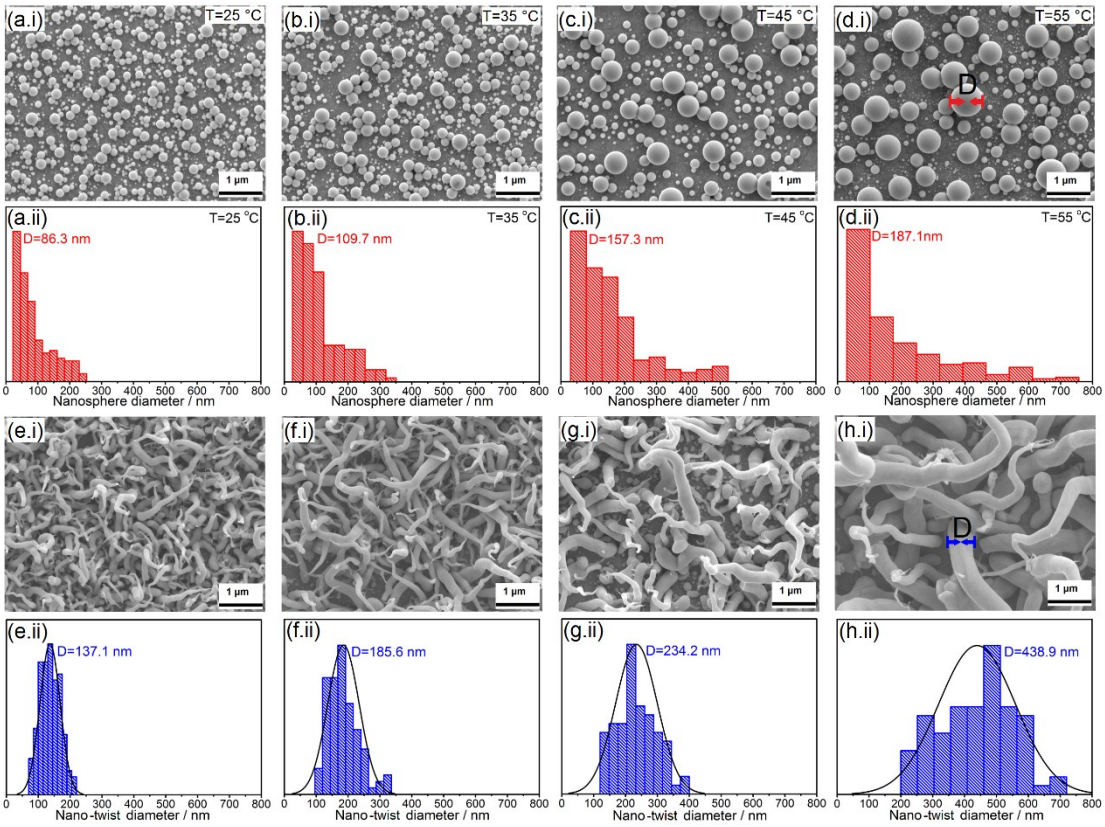

Fig. S7. The morphology and corresponding size distribution of Ga nanospheres deposited at temperature of 25 (a), 35 (b), 45 (c), (d) 55 °C. (e-h) FESEM images and bottom diameter size distribution of $Ge_{0.90}Ga_{0.10}$ nano-twist after electrodeposition Ge for 300 s at 60 °C.

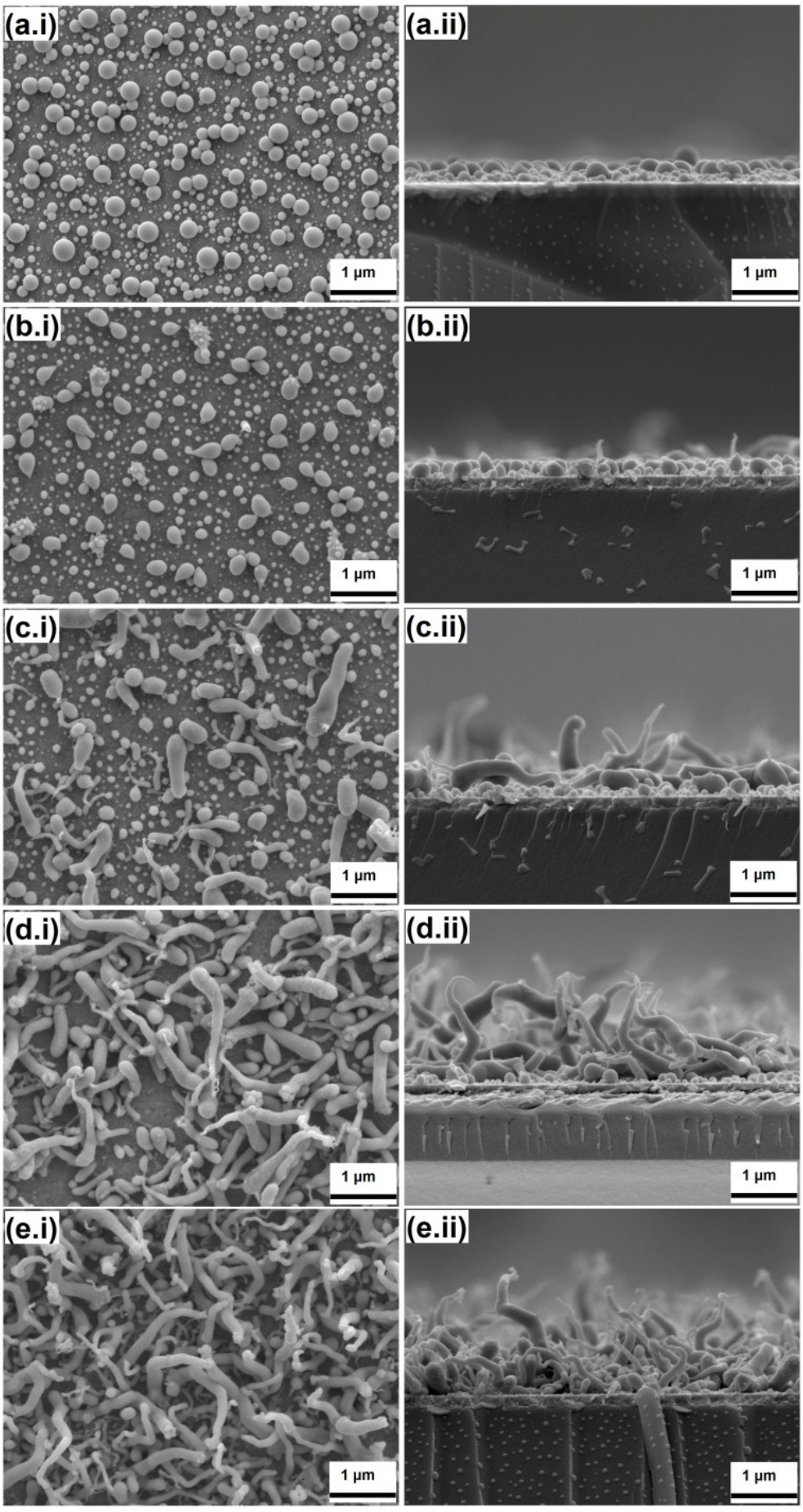
(a.i)
1 µm
(a.ii)
1 µm
(b.i)
1 µm
(b.ii)
1 µm
(c.i)
1 µm
(c.ii)
1 µm
(d.i)
1 µm
(d.ii)
1 µm
(e.i)
1 µm
(e.ii)
1 µm

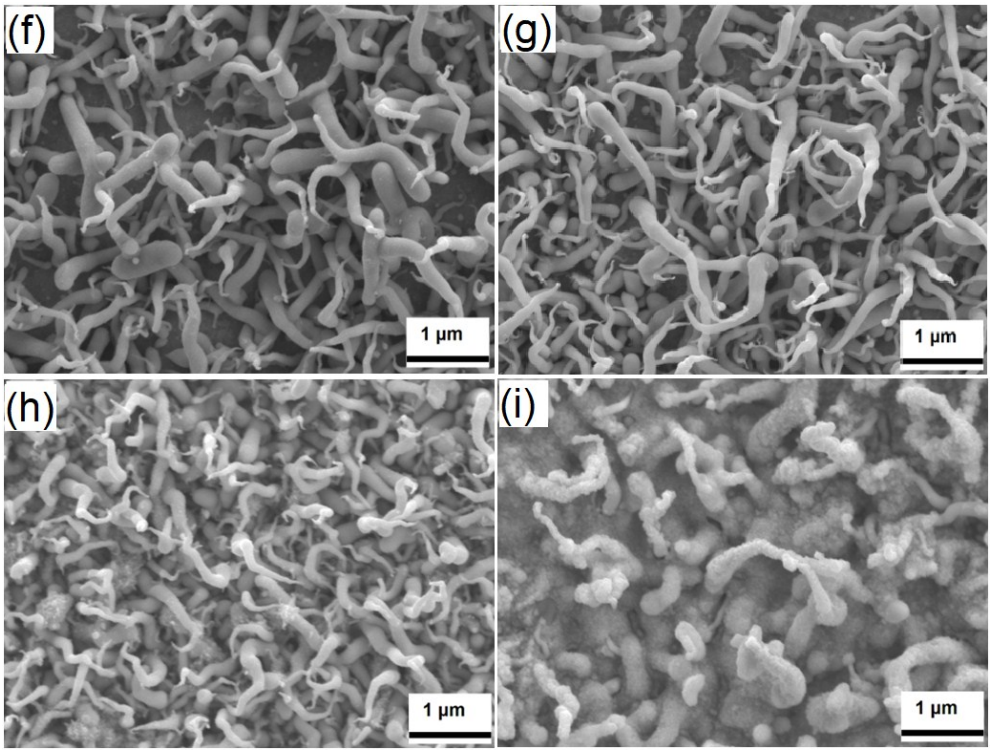

Fig. S8. FESEM images of the top and cross-section view of Ga and Ge deposits. (a.i, a.ii) Ga electrodeposited for 30 s, (b.i, b.ii) Ge electrodeposited for 10 s, (c.i, c.ii) 30s, (d.i, d.ii) 60 s, (e.i, e.ii) 90 s. (f) 120s, (g) 150 s, (h) 450 s, (i) 600 s.

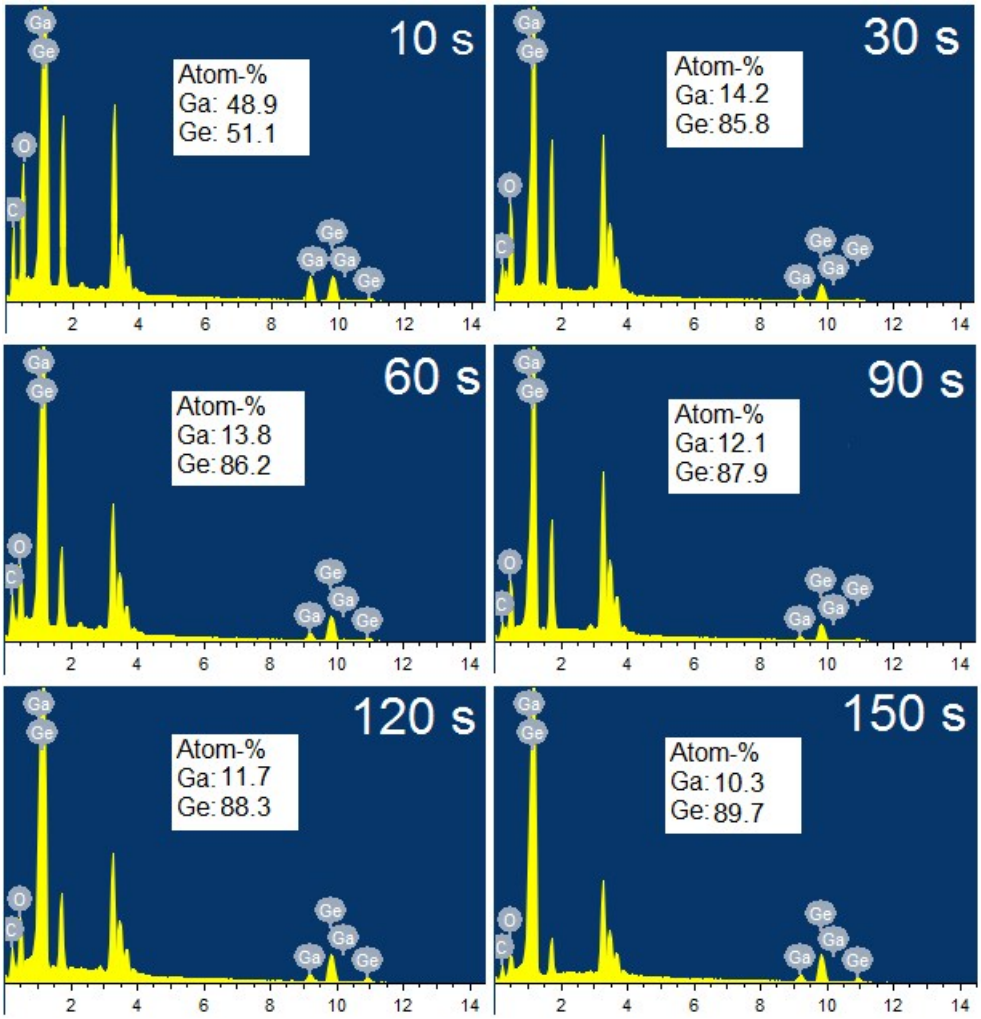

Fig. S9. EDX results of Ge deposits for different deposition time.

Table S1. Atomic ratio of Ga/(Ga+Ge) calculated based on EDX results.

Electrodeposition time of Ge	**10 s**	**30 s**	**60 s**	**90 s**	**120 s**	**150 s**
Ga/(Ga+Ge)	48.9%	14.2%	13.8%	12.1%	11.7%	10.3%
Ge/(Ga+Ge)	51.1%	85.8%	86.2%	87.9%	88.3%	89.7%

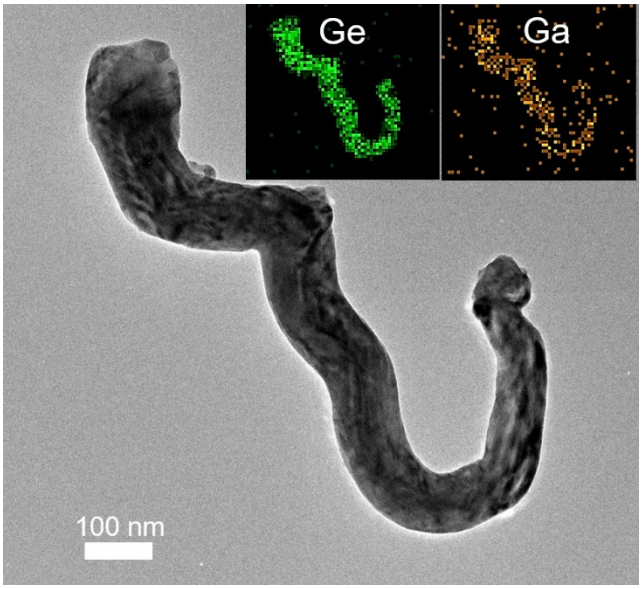

Fig. S10. TEM image and corresponding elemental mapping image of a nano-twist.

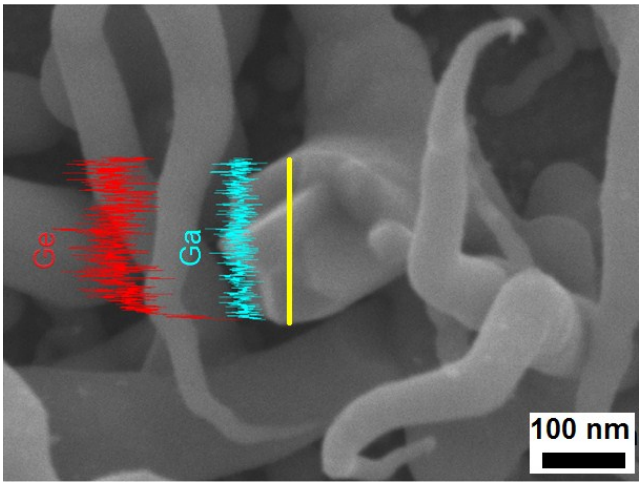

Fig. S11. Line scan profile along the $Ge_{0.90}Ga_{0.10}$ nano-twist diameter.

Table S2 shows a comparison of $Ge_{0.90}Ga_{0.10}$ nano-twist electrode with previously published literature on Ge-based nanowires anodes. The very high capacity of 819 mA h g^{-1} at 16 A g^{-1} is highest for the Ge-based nanowires listed in Table S2. The solution-grown Ge nanowires have the discharge capacity of 900 mA h g^{-1} at 16 A g^{-1} when charged at 1.6 A g^{-1}; however, low charge rate always leads to high discharge capacity. When it was charged/discharged at the same current density of 3.2 A g^{-1}, a rate capability lower than 1000 mA h g^{-1} was observed.

Table S2. A comparison of $Ge_{0.90}Ga_{0.10}$ nano-twist electrode with previously published literature on Ge-based nanowires anodes.

Material	Method	Need binder or conductive carbon	Cycling performance (mA h g^{-1})	Rate capability (mA h g^{-1})	Ref.
Strain-released Ge nanowires	Ionic liquid electrodeposition and annealing treatment	NO	1200 after 200 cycles at 0.16 A g^{-1}	325 at 16 A g^{-1}	S4
Ge nanowires	VLS	NO	1141 after 20 cycles at 0.08 A g^{-1}	NA	14
Ge/C nanowires on carbon nanofibers	VLS	YES	820 after 100 cycles at 0.16 A g^{-1}	484 at 16 A g^{-1}	S5
Ge/C nanowires	SLS	YES	~700 after 100 cycles at 0.8 A g^{-1}	700 at 9.6 A g^{-1}	S6
Dodecanethiol-passivated Ge nanowires	Supercritical fluid-liquid-solid (SFLS)	YES	1130 after 100 cycles at 0.16 A g^{-1}	~555 at 17.6 A g^{-1}	S7
Sn-seeded Ge nanowires	VLS	NO	~900 after 1100 cycles at 0.8 A g^{-1}	538 at 16 A g^{-1}	S8
Graphene/Ge nanowires	VLS	YES	1059 after 200 cycles at 6.4 A g^{-1}	~800 at 16 A g^{-1}	S9
Graphene/Ge nanowires	Arc-discharge	YES	~1400 after 50 cycles at 1.6 A g^{-1}	781 at 16 A g^{-1}	S10
Ge nanowires	Ec-LLS	NO	970 after 20 cycles at 1.6 A g^{-1}	NA	33
Ge nanowire	Solution-grown	YES	1248 after 100 cycles at 0.16 A g^{-1}	900 discharged at 16 A g^{-1} when Charged at 1.6 A g^{-1}	S11
$Ge_{0.90}Ga_{0.10}$ nano-twist	In-situ Ga-Alloying ionic liquid electrodeposition	NO	1146 after 150 cycles at 0.32 A g^{-1}	819 at 16 A g^{-1}	This work

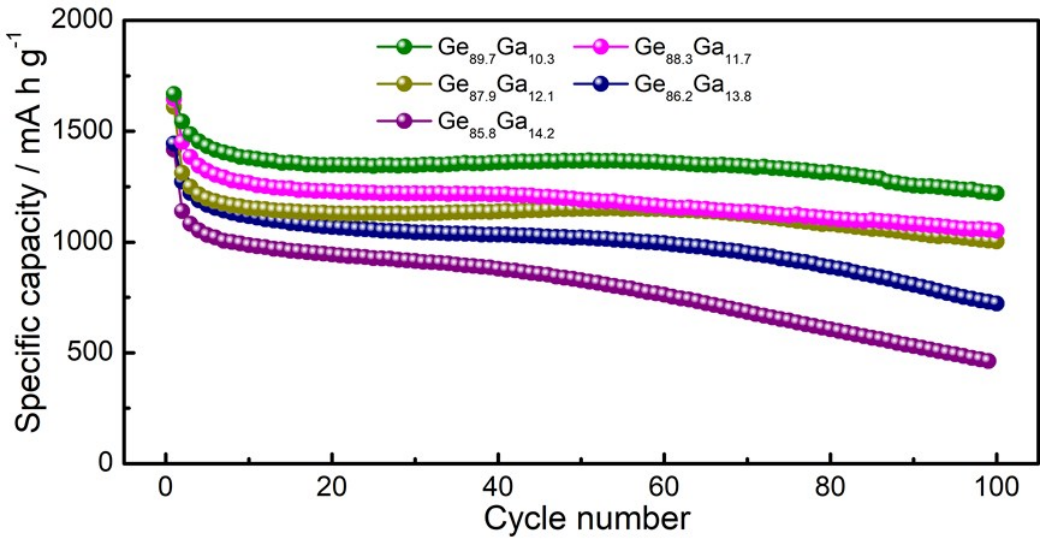

Fig. S12. Cycling performance of different Ga content nano-twists at a current density of o.32 A g^{-1}.

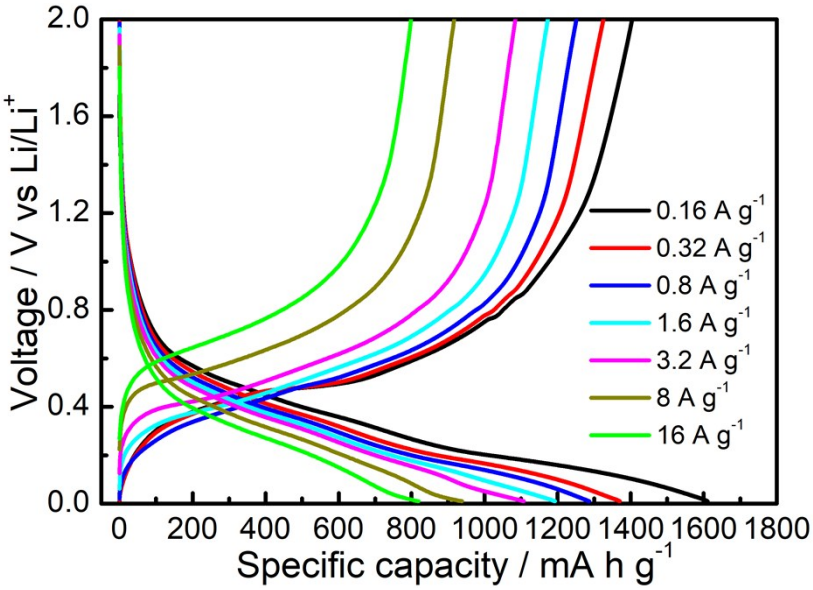

Fig. S13. The corresponding charge-discharge voltage profiles of $Ge_{0.90}Ga_{0.10}$ nano-twist at different current densities.

For comparison, the cycling performance and rate capability of the Ge-nano-tree were measured, and the results are shown in Fig. S14(a) and (b), respectively. The nano-tree had the initial discharge capacity of 1427 mA h g^{-1} with the capacity retention of 796 mA h g^{-1} after 100 cycles when cycled at 0.32 A g^{-1}. The discharge capacity of the nano-tree at 16 A g^{-1} was 98 mA h g^{-1}, which was much lower than that of the $Ge_{0.90}Ga_{0.10}$ nano-twist. The good capacity retention of the $Ge_{0.90}Ga_{0.10}$ nano-twist indicated that this nano-twist had a relatively stable structure than the Ge nano-tree. The structural changes of the nano-twists after 150 cycles and those of Ge nano-trees after 100 cycles were observed (Fig. S15). After 150 cycles, the nano-twist exhibited a stable porous network structure. This structure can provide continuous electrical conduction and ion transport paths, thus facilitating high rate of Li-ion diffusion, stress release and cycle stability. [S12] Contrary to nano-twists, the Ge nano-tree suffers significant pulverization with the fracture of branches from the trunk.

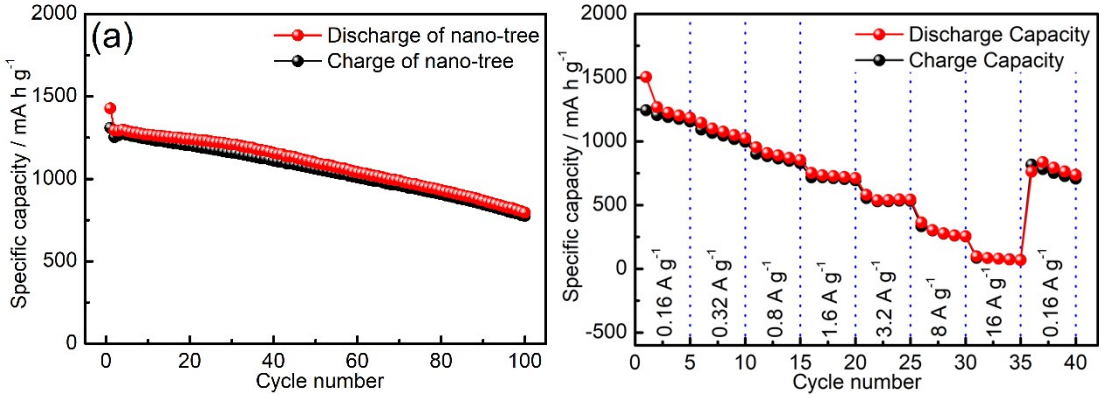

Fig. S14. (a) Cycling behavior of the Ge nano-tree anode at a current density of 0.32 A g^{-1}. (b) Rate capability of the Ge nano-tree.

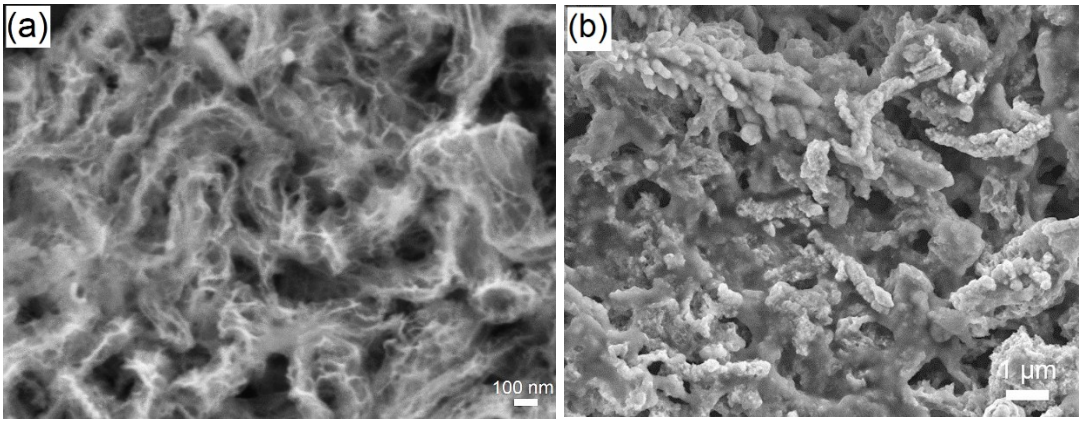

Fig. S15. (a) FESEM image of $Ge_{0.90}Ga_{0.10}$ nano-twist after 150 cycles. (b) FESEM image of Ge nano-tree after 100 cycles.

Supplementary References:

[S1] J. Xie, N. Imanishi, T. Zhang, A. Hirano, Y. Takeda and O. Yamamoto, *Electrochim. Acta*, 2009, **54**, 4631-4637.

[S2] H. G. Jung, J. Hassoun, J. B. Park, Y. K. Sun and B. Scrosati, *Nat. Chem*., 2012, **4**, 579-585.

[S3] Z. Xu, J. Yang, T. Zhang, Y. Nuli, J. Wang and S. I. Hirano, *Joule*, 2018, **2**, 950-961.

[S4] J. Hao, Y. Yang, J. Zhao, X. Liu, F. Endres, C. Chi, B. Wang, X. Liu and Y. Li, *Nanoscale*, 2017, **9**, 8481-8488.

[S5] W. Li, M. Li, Z. Yang, J. Xu, X. Zhong, J. Wang, L. Zeng, X. Liu, Y. Jiang, X. Wei, L. Gu and Y. Yu, *Small*, 2015, **11**, 2762-2767.

[S6] M. H. Seo, M. Park, K. T. Lee, K. Kim, J. Kim and J. Cho, *Energy Environ. Sci*., 2011, **4**, 425-428.

[S7] F.W. Yuan, H. J. Yang, H. Y. Tuan, *Acs Nano*, 2012, **6**, 9932-9942.

[S8] T. Kennedy, E. Mullane, H. Geaney, M. Osiak, C. O'Dwyer, K. M. Ryan, *Nano Lett*., 2014, **14**, 716-723.

[S9] H. Kim, Y. Son, C. Park, J. Cho, H. C. Choi, *Angew. Chem. Int. Ed*., 2013, **52**, 5997-6001.

[S10] C. Wang, J. Ju, Y. Yang, Y. Tang, J. Lin, Z. Shi, R. P. S. Han, F. Huang, *J. Mater. Chem. A*, 2013, **1**, 8897-8902.

[S11] A. M. Chockla, K. C. Klavetter, C. B. Mullins and B. A. Korgel, *ACS Appl. Mater. Interfaces*, 2012, **4**, 4658-4664.

[S12] X. H. Liu, S. Huang, S. T. Picraux, J. Li, T. Zhu and J. Y. Huang, *Nano Lett*., 2011, **11**, 3991-3997.